European Journal of Pharmaceutical Sciences 137 (2019) 105010

Contents lists available at ScienceDirect

European Journal of Pharmaceutical Sciences

journal homepage: www.elsevier.com/locate/ejps

Synthesis and anti-cancer activity of **ND-646** and its derivatives as acetyl-CoA carboxylase 1 inhibitors

En-Qin Li[a,1], Wei Zhao[b,c,1], Chenxi Zhang[d,1], Lu-Zhe Qin[a], Sheng-Jie Liu[a], Zhi-Qi Feng[a], Xiaoan Wen[a,*], Cai-Ping Chen[a,*]

[a] Jiangsu Key Laboratory of Drug Discovery for Metabolic Disease and State Key Laboratory of Natural Medicines, China Pharmaceutical University, 24 Tongjia Xiang, Nanjing 210009, China
[b] Department of Clinical Biochemistry, School of Laboratory Medicine, Chengdu Medical College, Chengdu 610050, China
[c] Department of Respiratory Medicine, The First Affiliated Hospital of Chengdu Medical College, Chengdu 610050, China
[d] Central Laboratory, Nanjing Chest Hospital, Medical School of Southeast University, Nanjing, Jiangsu Province 210029, China

ARTICLE INFO

Keywords:
Acetyl-CoA carboxylase
De novo fatty acid synthesis
Lung cancer

ABSTRACT

Acetyl-coA carboxylase 1 (ACC1) is the first and rate-limiting enzyme in the *de novo* fatty acid synthesis (FASyn) pathway. In this study, through public database analysis and clinic sample test, we for the first time verified that *ACC1* mRNA is overexpressed in non-small-cell lung cancer (NSCLC), which is accompanied by reduced DNA methylation at CpG island S shore of *ACC1*. Our study further demonstrated that higher *ACC1* levels are associated with poor prognosis in NSCLC patients. Besides, we developed a novel synthetic route for preparation of a known ACC inhibitor **ND-646**, synthesized a series of its derivatives and evaluated their activity against the enzyme ACC1 and the A549 cell. As results, most of the tested compounds showed potent ACC1 inhibitory activity with IC_{50} values 3–10 nM. Among them, compounds **A2**, **A7** and **A9** displayed strong cancer inhibitory activity with IC_{50} values 9–17 nM by impairing cell growth and inducing cell death. Preliminary SAR analysis clearly suggested that (*R*)-configuration and amide group were vital to ACC1 and A549 inhibition, since compound **(*S*)-A1** (the enantiomer of **ND-646**) had poor activity of ACC1 inhibition and the carboxylic acid **ND-630** almost lost anticancer effect on A549 cells. Collectively, these findings indicate that ACC1 is a potential biomarker and target for non-small-cell lung cancer, and **ND-646** and its derivatives as ACC1 inhibitors deserve further study for treatment of NSCLC.

1. Introduction

Cancer cells showed an extraordinary need of biological macromolecules including nucleic acids, proteins, and lipids to support continuous proliferation (Vander Heiden et al., 2009). Therefore, cancer cells tend to reprogram their metabolism to meet such need, resulting in alterations in glucose and glutamine metabolism (Martinez-Outschoorn et al., 2017; Cairns and Mak, 2016). In addition, a number of cancers show an increase in *de novo* fatty acid synthesis (FASyn) (Medes et al., 1953; Currie et al., 2013; Menendez and Lupu, 2007; Zadra et al., 2019). It has been demonstrated that decrease of FASyn by genetic approaches or chemical compounds inhibited tumor growth (Chajes et al., 2006; Svensson and Shaw, 2016). Acetyl-CoA carboxylase (ACC) mediates the first step of FASyn by carboxylation of acetyl-CoA to form malonyl-CoA and functions as a rate-limiting enzyme in FASyn. Two isoforms of ACC with distinct subcellular distribution and physiological roles have been identified, of which the cytosolic isoform ACC1 is predominant in control of the fatty acid synthesis, while the mitochondrial isoform ACC2 mainly regulates the fatty acid oxidation through inhibition of carnitine palmitoyltransferase I by localized malonyl-CoA production (McGarry et al., 1978). With regard to cancer progression, current research focus is on ACC1 but not ACC2, though the both two isoforms are involved in lipid metabolism (Braig, 2018; Wang et al., 2015). Moreover, it was reported that *ACC1* was the dominant isoform in several tested human lung cancer cell lines, while *ACC2* was nearly undetectable (Svensson et al., 2016). Upregulation of *ACC1* mRNA or protein was observed in a number of cancers, including breast, liver and prostate cancers (Chin et al., 2006; Swinnen et al., 2000). *ACC1* silencing or deletion in cancer cells led to a loss of FASyn and cell growth inhibition, which were rescued by addition of

* Corresponding authors.
E-mail addresses: wxagj@126.com (X. Wen), caiping.chen@cpu.edu.cn (C.-P. Chen).
[1] These authors contributed equally.

https://doi.org/10.1016/j.ejps.2019.105010
Received 22 March 2019; Received in revised form 9 July 2019; Accepted 15 July 2019
Available online 17 July 2019
0928-0987/

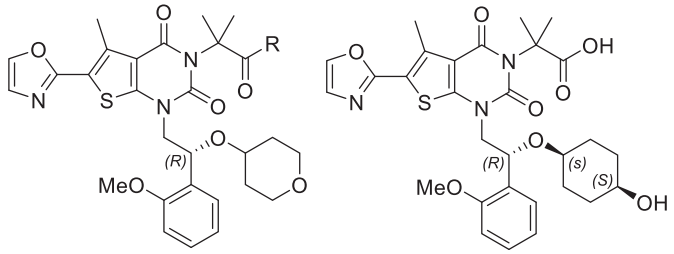

Fig. 1. Structures of **ND-630**, **ND-646** and **ND-654.**

exogenous palmitate (Chajes et al., 2006; Svensson et al., 2016; Brusselmans et al., 2005).

A couple of ACC inhibitors such as 5-(tetradecyloxy)-2-furoic acid (TOFA), soraphen A and BAY ACC002 have been reported to show anti-tumor activity (Petrova et al., 2017; Beckers et al., 2007). Very recently, Harriman et al. identified a series of potent and highly specific allosteric ACC dimerization inhibitors, *e.g.* **ND-630**, **ND-646** and **ND-654** (Fig. 1) (Svensson et al., 2016; Harriman et al., 2016; Lally et al., 2019). These dimerization inhibitors bind to the key residues Arg172 (ACC1) and Arg277 (ACC2) that the AMPK-phosphorylated serine interacts with, thus mimicking the physiological inhibition of ACC dimerization and enzymatic activity by AMPK (Svensson and Shaw, 2016; Harriman et al., 2016). Both **ND-630** and **ND-654** were shown to be liver specific. The former could reduce hepatic steatosis, improve insulin sensitivity and modulate dyslipidemia, and is currently in clinical trial phase II for treatment of nonalcoholic fat liver disease (Harriman et al., 2016). The latter was able to suppress lipogenesis and hepatocellular carcinoma (Lally et al., 2019). However, **ND-646**, the amide derivative of **ND-630**, was shown to be broadly distributed, significantly inhibit fatty acid synthesis in lung tumors and strikingly suppress lung tumor growth both *in vitro* and in mouse models (Svensson et al., 2016). **ND-646** was well tolerated in mice. Chronic **ND-646** treatment of tumor-bearing mice at the oral dose of 25 mg/kg twice daily or 50 mg/kg once daily for 31 days did not cause body weight lost, and at the higher dose of 50 mg/kg twice daily or 100 mg/kg twice daily for 6 weeks only reduced 10% body weights (Svensson et al., 2016).

In the present study, by public database analysis and clinic sample test, we found that *ACC1* mRNA is overexpressed in non-small-cell lung cancer (NSCLC) and higher expression of *ACC1* is significantly correlated with shorter progression free survival (PFS) in NSCLC patients. It suggests that ACC1 might be a promising predictive biomarker as well as a potential therapeutic target for NSCLC. Thus, we synthesized **ND-646** and a series of its derivatives, and evaluated their ACC1 inhibitory activity and anti-cancer activity in NSCLC.

2. Materials and methods

2.1. Clinical specimen collection

Sixty-three patients who received surgery at the department of respiratory medicine, the first affiliated hospital of Chengdu Medical College during 2015 to 2017 were included in this study. Lung specimens from cancer tissues and normal tissues (with > 5 cm distance from the tumor edge) were immediately frozen in liquid nitrogen and then stored at −80 °C until use. None of the patients received any chemotherapy or radiotherapy before surgery. The Research Ethics Committee of Chengdu Medical College approved this protocol and informed written consent was obtained from all the participants.

2.2. RNA collection, reverse transcription, and quantitative RT-PCR (qRT-PCR)

RNA was extracted using PureLink™ RNA Mini Kit (Cat no. 12183025, Thermo Fisher Scientific, Carlsbad, CA, USA) following manual and then reverse-transcribed by random primers using TaKaRa reverse transcription kit (Dalian, China). Real-time PCR (qRT-PCR) was carried out, using SYBR Green in an ABI 7500 StepOne Plus Real Time PCR instrument (Applied Biosystems, USA). The relative expression level of each target gene was normalized to β-actin in one sample. Primers used in our study were as follows: AAC1: forward primer: 5′-ATG TCT GGC TTG CAC CTA GTA-3′ and reverse primer: 5′-CCC CAA AGC GAG TAA CAA ATT CT-3′; and β-actin: forward primer: 5′-CAT GTA CGT TGC TAT CCA GGC-3′ and reverse primer: 5′-CTC CTT AAT GTC ACG CAC GA-3′.

2.3. hACC1 enzyme inhibition assays

IC_{50} values of compounds inhibition on hACC1 were assessed by WuXi App Tec (Shanghai) Co., Ltd. using a luminescent ADP detection assay (ADP-Glo™ Kinase Assay Kit; Promega) according to previous reported by Harriman et al. (Harriman et al., 2016), using recombinant hACC1 (BPS Biosciences Catalog #50200), as the source of enzyme.

2.4. Cell lines and culture

A549 and H1975 Cells were purchased from the Cell Bank of Shanghai Institute of Cell Biology, Chinese Academy of Sciences. A549 cells and H1975 cells were maintained in DMEM medium and modified RPMI-1640 medium respectively, supplemented with 10% fetal bovine serum (FBS), 100 μg/mL penicillin and 100 U/mL streptomycin in a 5% CO_2 humidified incubator at 37 °C.

2.5. Cell viability assay

Cells were seeded at about 500 cells/well (100 μL) in 96-well plates in medium containing regular 10% FBS overnight for attachment. After being washed once with PBS, cells were switched into medium containing 20% delipidated FBS (Gemini #900–123) with concentrations of compounds. After incubating for another 7 days, cell viability were determined by MTT assay as previously described (Huang et al., 2018; Song et al., 2016; Chen et al., 2019). Briefly, 20 μL of MTT solution (3-(4,5-dimethyl thiazol −2-yl)-2,5-di phenyl tetrazolium bromide) were added into each well and incubated for 4 h. The formed insoluble formazan was dissolved with 150 μL of DMSO and then measured colorimetrically at 490 nm by Enspire (PekinElmer, Waltham, MA, USA). The viability of control group was set as 100%, and the values of other groups were represented as percentages of the control group. The IC_{50} values were calculated through nonlinear regression analysis by using GraphPad Prism 5.0 software.

2.6. Proliferation/cytotoxicity assays

Cells were seeded at 300 cells/well in 96-well plates and treated with ACC1 inhibitors in delipidated FBS as mentioned above. At the indicated time points after treatment, cell numbers were determined using an Opera Phenix High Content Screening System (Perkin-Elmer, Waltham, MA, USA) through digital phase contrast imaging or DAPI staining toward the end treatment. Afterwards, cells were subjected to cell death analysis by annexin V/PI staining. Briefly, cells in 96-well plate were washed with PBS twice and stained with annexin V/PI (A211–02, Vazyme, Nanjing, China) according to the manufacture's instruction. The fluorescence and brightfield were visualized with the Opera Phenix High Content Screening System (Perkin-Elmer, Waltham, MA, USA).

For regular medium, cells were seeded at 2000 cells/well in 6-well

plates in medium containing regular 10% FBS and were treated with ACC1 inhibitors (1 μM) or DMSO vehicle for control the next day. Medium containing compounds were refreshed at days 6 post treatment, before cell death became obvious. Then, cells were incubated for another 6 days. During the period of culture, wet condition was always ensured.

2.7. Western blot assay

To assess the effects of ACC inhibitors on ACC phosphorylation, A549 cells were seeded at a 3×10^5/well in a 6-well plate. After 24 h, cells were treated with compounds (1 μM) or vehicle control for 24 h. After washed with ice-cold PBS, cells were lysed by RIPA buffer containing protease and phosphatase inhibitors (Millipore). Equal amounts of protein were subjected to Western blot assay as previously described (Chen et al., 2019; Chen et al., 2015). Primary antibodies against ACC (#3676S) and p-ACC (#3661S) were purchased from Cell Signaling Technology.

2.8. Establishment of Osi-resistant NCI-H1975 cells

Osimertinib resistance H1975 cells were established by exposing H1975 cells to gradually increasing concentrations of osimertinib from 0.05 μM to 5 μM. Cells became resistant to Osi after approximately 6 months, reflected by appearing a normal exponential growth rate at 5 μM osimertinib. The cell line was routinely cultured in the presence of 5 μM osimertinib. The newly established OSI-resistant cells were termed as H1975/OsiR cells. During the establishment of H1975/OsiR cells, the parental H1975 cells were always kept in drug-free medium in parallel for control.

2.9. Chemistry

^{1}H NMR spectra was recorded on an ACF* 300Q Bruker or ACF* 500Q Bruker spectrometer. Low- and high-resolution mass spectra (LRMS and HRMS) were recorded in electron impact mode. The mass analyzer type used for the HRMS measurements was TOF. Reactions were monitored by TLC on silica gel 60 F254 plates (Qingdao Ocean Chemical Company, China). Column chromatography was carried out on silica gel (200–300 mesh, Qingdao Ocean Chemical Company, China). Data for 1H NMR are recorded as follows: chemical shift (δ, ppm), multiplicity (s = singlet, d = doublet, t = triplet, m = multiplet or unre solved, br = broad singlet, coupling constant (s) in Hz, integration). Commercially available reagents and solvents were used without further purification.

3. Results

3.1. ACC1 expression is upregulated in non-small-cell lung cancer

ACC1 has been reported to be upregulated in breast, liver and prostate cancers (Chin et al., 2006; Swinnen et al., 2000). However, so far as we know, there was no report on mRNA levels of *ACC1* in lung cancer tissues, despite the phosphorylation status of ACC has been analyzed previously (Rios Garcia et al., 2017; Carretero et al., 2007). In this study, by using the Oncomine™ Platform (Okayama et al., 2012; Hou et al., 2010), we found that *ACC1* mRNA expression is significantly increased in both lung adenocarcinoma (LUAD) and lung squamous cell carcinoma (LUSC) compared to normal lung tissues (Fig. 2A). Consistently, we observed higher levels of *ACC1* in NSCLC tissues than that in normal lung tissues by qRT-PCR analysis of clinic samples (Fig. 2B). According to a previous study on chicken, alterated expression of *ACC1* might be associated with the epigenetic modification (Liu et al., 2016). In the present study, by using the MethHC database (Huang et al., 2015), we observed that DNA methylation at CpG island S shore of *ACC1* reduced in both LUAD and LUSC (Fig. 2C). CpG island shores, composed of N shore and S shore, are recently coined regions with relatively lower CpG density, located < 2 kb flanking CpG islands (Portela and Esteller, 2010). The methylation of CpG island shores is reported to be closely associated with genes transcriptional inactivation (Portela and Esteller, 2010). The DNA methylation rates of other regions, including the promoter, CpG islands, 5'UTR, 3'UTR, enhancer and N shore of *ACC1* are not significantly different between lung cancers and normal lungs (data not shown). Therefore, the increased *ACC1* mRNA abundance in lung cancers might result from the reduced DNA methylation at CpG island S shore.

To identify whether the mRNA level of *ACC1* is clinically relevant in lung cancer, we examined correlations between *ACC1* expression and survival of lung cancer patients using an online tool (http://www.kmplot.com) (Gyorffy et al., 2013). As results shown, individuals with high *ACC1* levels exhibited shorter progression-free survival (PFS) compared to those with low levels (Fig. 1D). Collectively, ACC1 might be a potential prognostic biomarker for NSCLC.

3.2. Synthesis of ND-646 and its derivatives

We ever attempted to synthesize **ND-646** according to the patent published procedure (Harriman et al., 2013), but encountered a lot of difficulties. Thus, we designed a novel 15-step route as depicted in Scheme 1. The intermediate **6** was prepared from the starting material **1** *via* 5 steps same as described in the patent(Harriman et al., 2013). Compound **6** was reacted with *o*-methoxyacetophenone bromide, followed by hydrolysis to give the intermediate **8**. The carboxylic group of **8** was protected with TBDPS, and the carbonyl group was reduced by $NaBH_4$ and brominated through the Apple Reaction. The resulting bromide **11** was treated with tetrahydropyranol and MgO/Mg_2SO_4 to give the ether **12**, which took place a Stille coupling reaction with 2-(tripropylstannml)-1,3-oxazole in the presence of PPh_3 and was subsequently treated by TBAF for removal of TBDPS to achieve the key racemic acid **14**. The racemate **14** was successfully separated by chiral preparative HPLC to offer a pair of enantiomers **ND-630** and **(*S*)-14** with *ee* > 98%. Finally, **ND-630** was converted to **ND-646** by ammonium hydroxide under T3P.

Reagents and conditions: (f) 2-bromo-2′-methoxyacetophenone, K_2CO_3, DMF, rt., overnight, 75%; (g) TFA, DCM, r.t., 1 h; (h) TBDPSCl, Imidazole, THF, rt., overnight, 83%; (i) $NaBH_4$, THF, rt., 5.5 h, 66%; (j) CBr_4, PPh_3, THF, 0 °C-r.t., overnight, 37%; (k) MgO, $MgSO_4$, tetrahydro-4- pyranol, 80 °C, 10 h, 46%; (l) 2-(tripropylstannml)-1,3-oxazole, PPh_3, toluene, 110 °C, 17 h, 41%; (m) TBAF, THF, rt., 1 h, 79%; (n) chiral preparative HPLC, > 98% ee; (o) $NH_3{\cdot}H_2O$, T3P, DCM, 10 h, 40%.

Treatment of **14** and **(*S*)-14** by diverse amines or alcohols under the coupling reagents HOBT/EDCI or T3P offered a series of racemic derivatives **A1**~**A12** and an optically pure amide **(*S*)-A1**, that is, the enantiomer of **ND-646** (see Supporting Information).

3.3. ACC1 inhibitory activity of ND-646 and its derivatives

The ACC1 inhibitory activity was tested according to the previously reported method (Harriman et al., 2016). As shown in Table 1, **ND-646** and its precursor **ND-630** displayed very strong potency of hACC1 inhibition, respectively with their IC_{50} values of 2.89 nM and 2.39 nM, identical to the literature data 3.5 nM [13] and 2.1 nM (Harriman et al., 2016). The racemate of **ND-646**, namely compound **A1**, also exhibited pretty good potency (IC_{50} = 5.89 nM), while the enantiomer of **ND-646**, namely compound **(*S*)-A1**, showed poor activity (IC_{50} = 1156 nM). The other compounds also exhibited quite strong inhibitory activity (IC_{50} < 23 nM), among which **A6** was the best (IC_{50} = 3.21 nM).

3.4. Anticancer activity of ND-646 and its derivatives against A549 cells

ND-646 and its derivatives were evaluated by cell viability assay for

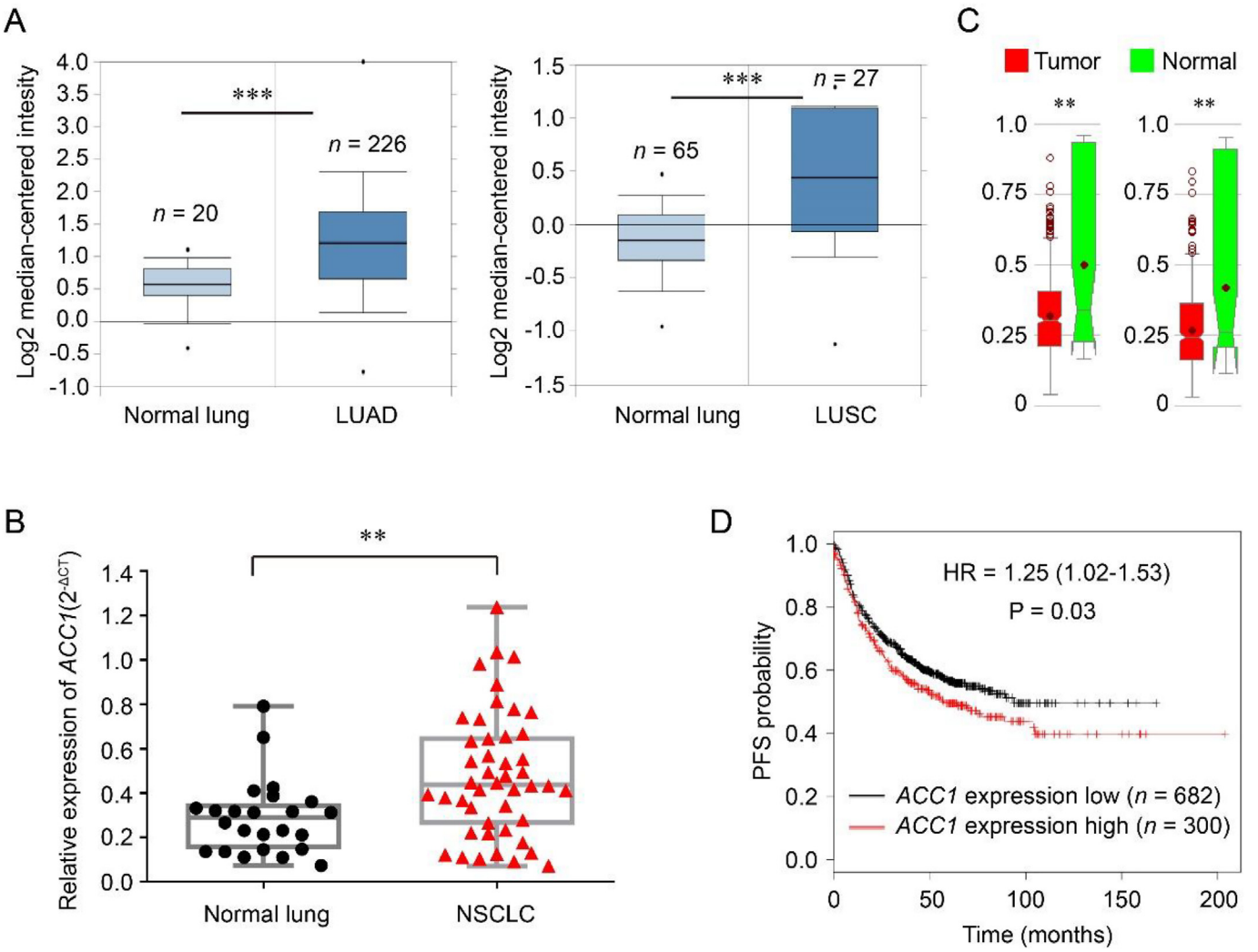

Fig. 2. *ACC1* expression is upregulated in lung cancers and higher *ACC1* levels predict a poor outcome. (A) Analysis of human *ACC1* expression in LUAD (left) and LUSC (right) as well as control normal lung samples, using Oncomine database (www.oncomine.org). ***$P < 0.001$ (Student's *t*-test). (B) Box whisker plot presenting the mean (min to max) value of *ACC1* mRNA expression levels in 46 human NSCLC tumors and 24 adjacent normal lung tissues by qRT-PCR. **$P < 0.01$ (Mann Whitney test). (C) The methylation rate at S Shore of *ACC1* is significantly reduced in both LUAD and LUSC compared with normal lung tissues according to the MethHC database (http://methhc.mbc.nctu.edu.tw/php/diffMeth.php).**$P < 0.005$.(D) Kaplan-Meyer plots showing progression free survival (PFS) in lung cancers. Patients with higher *ACC1* expression associated with shorter PSF compared with those with low *ACC1* expression ($P = 0.03$). Cox's proportional hazards model was used to calculate hazard ratio (HR). HR > 1 indicates that patients with high *ACC1* expression exhibited a poor prognosis.

their anticancer activity against A549 cells, which expressed the highest *ACC1* levels among the three NSCLC cell lines that we detected (Fig. S1).

To best reflect the FASyn inhibition on tumor cell viability, cells were cultured in delipidated fetal bovine serum (FBS) (Svensson et al., 2016). The IC_{50} values are summarized in Table 1. Six compounds showed strong proliferation inhibitory activity in A549 cells ($IC_{50} < 100$ nM). Among them, the cyclohexyl amide **A7** displayed the best activity ($IC_{50} = 9.4 \pm 3.2$ nM). The methyl amide **A2** ($IC_{50} = 16.8 \pm 3.8$ nM) and the hydroxyethyl amide **A9** ($IC_{50} = 23 \pm 4.6$ nM) showed potency comparable to **ND-646** ($IC_{50} = 16.2 \pm 10.6$ nM). However, the enantiomer of **ND-646**, namely **(*S*)-A1**, showed almost no anticancer activity ($IC_{50} > 50{,}000$ nM), consistent with its low hACC1 inhibitory activity. Surprisingly, **ND-630** also displayed disappointed anticancer activity ($IC_{50} > 20{,}000$ nM) in spite of its hACC1 inhibitory activity strong as **ND-646**, maybe due to poor uptake in A549 cells, since **ND-630** was reported highly liver specific (Harriman et al., 2016).

Prelimilary SAR analysis revealed that when the R group was a chain, a long chain seemed unfavourable, since the anticancer activity of **A2**, **A3** and **A4** gradually decreased. Strangely, when it was a ring, a large ring seemed favourable, since the activity of **A5**, **A6** and **A7** gradually increased. Besides, introduction of hydroxy group had effects on the potency of anticancer activity. The alcohols **A9** and **A10** were much more active than the corresponding non-alcohols **A3**, **A4** and **A7**, while the 4-hydroxypiperidine **A11** was less active than the piperidine **A7**.

3.5. Effect of **ND-646** and its derivatives on ACC phosphorylation

Crystallographic study has demonstrated that **ND-646** binds to the same residues as the AMPK-phosphorylated serines in ACC1 and ACC2 interact with, mimicking the physiological dimerization inhibition by AMPK. Reduction in AMPK-phosphorylated serines of ACC (p-ACC) has been used to reflect ACC engagement of ACC inhibitors (Svensson et al., 2016; Lally et al., 2019). Thus, we explored effects of compounds **A2**, **A7** and **A9** on *ACC* phosphorylation. It was found that similar with **ND-646**, these 3 compounds could eliminate p-ACC levels (Fig. 3), confirming their mechanism of action.

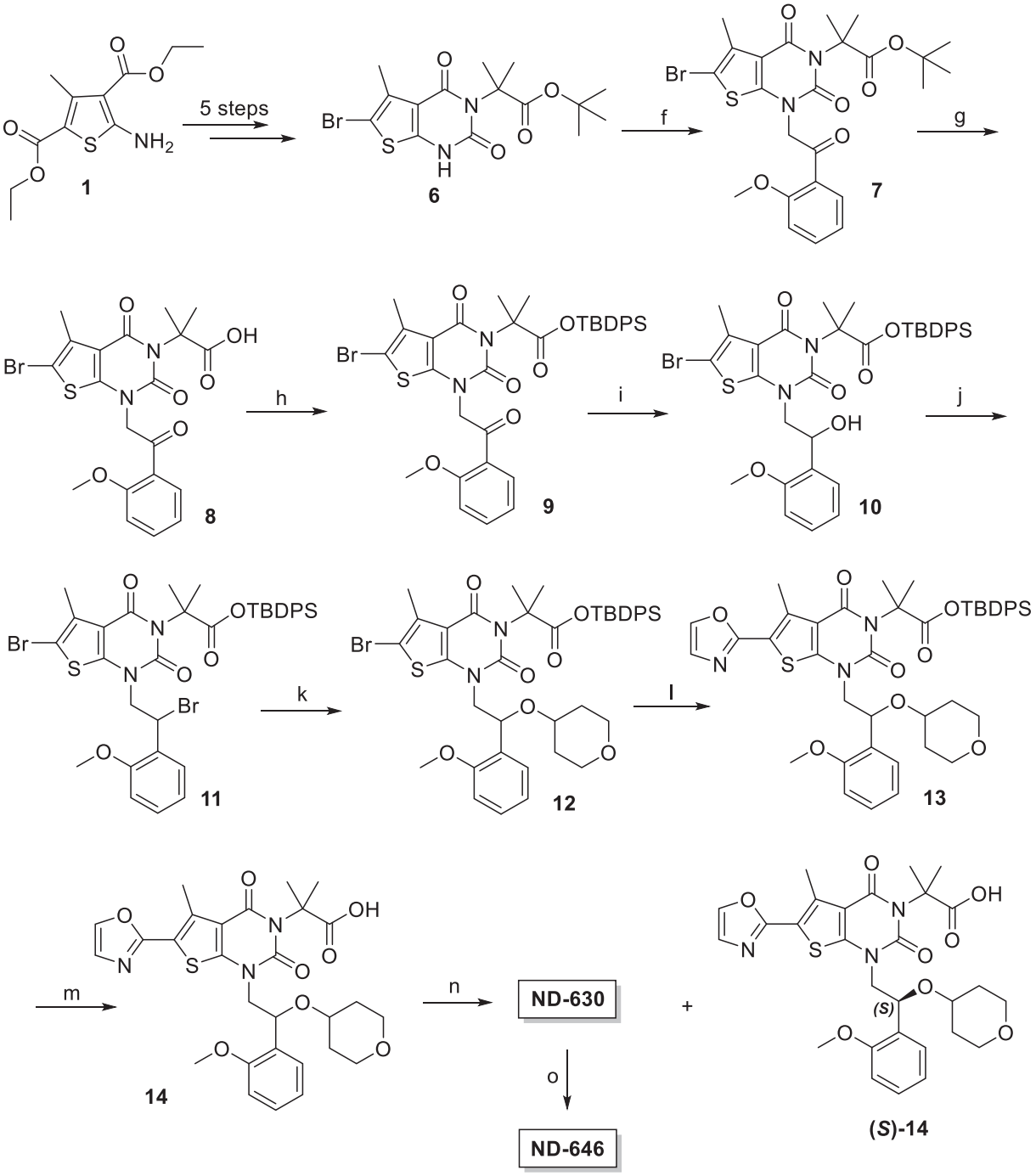

Scheme 1. Synthesis of **ND-646.**

3.6. ACC1 inhibitors impaired cell growth and caused cell death

To further understand the tumor inhibitory effects of the synthesized ACC1 inhibitors, we examined their effects on cell proliferation and cell death. Compounds **A2**, **A7** and **A9** time-dependently decreased the cell number of A549 cells, similar to **ND-646** (Fig. 4A and B). Moreover, annexin V-FITC/PI staining revealed that dying cells with annexin V-positive/PI- positive or Annexin V-negative/PI-positive, representing late apoptosis and necrosis respectively, were extensively seen after ACC1 inhibitors treatment for 7 days (Fig. 4C).

Notably, ACC1 inhibitors treatment of A549 cells grown in regular (not delipidated FBS) also inhibited cell growth and caused cell death, though it required longer time compared to that of cells in delipidated FBS (Fig. 4D).

3.7. Sensitivity to ACC1 inhibitors reduced in osimertinib-resistant H1975 cells

As is known, patients harboring mutations in epidermal growth factor receptor (EGFR), even if they initially could benefit from tyrosine kinase inhibitors (TKIs), later likely become resistant to such drugs including the third generation of TKI Osimertinib (Osi, also known as AZD9291) (Jiang et al., 2018; Romaniello et al., 2018). Treatment of TKI-resistant patients remains tremendously challenging. In the present study, we sought to verify whether ACC inhibitors have anticancer activity in Osi-resistant lung cancer cells. Hence, we established Osi-

Table 1
The hACC1 and A549 cell proliferation inhibitory activities of **ND646** and its derivatives.

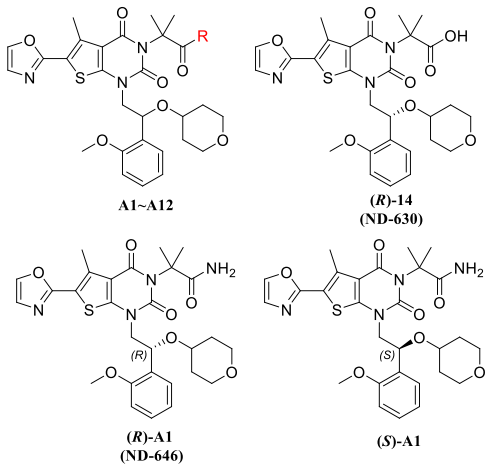

Compd	R	IC_{50} (nM) hACC1 inhibition	IC_{50} (nM)[a] against A549 cells
A1		5.89	117 ± 18
A2		6.69	16.8 ± 3.8
A3		8.90	1029 ± 488
A4		7.86	1967 ± 1227
A5		8.90	434 ± 21
A6		3.21	63.4 ± 11.8
A7		6.87	9.4 ± 3.2
A8		22.87	7231 ± 1902
A9		6.57	23.0 ± 4.6
A10	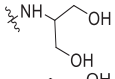	7.56	395 ± 214
A11	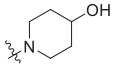	17.23	89.7 ± 31.4
A12	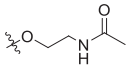	10.83	1300 ± 719
(*S*)-A1		1156	> 50,000
(*R*)-A1 ND-646		2.79	16.2 ± 10.6
ND-630		2.39	> 20,000

[a] The values were obtained from at least two independent experimental results and are given as mean ± standard deviation (SD).

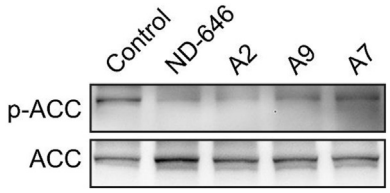

Fig. 3. ACC phosphorylation eliminated by **ND646**, **A2**, **A7** and **A9.**

resistant H1975 cells (H1975/OsiR) (Fig. 5A) and tested the cytotoxic activity of **ND-646**, **A2**, **A7** and **A9** on H1975/OsiR by MTT assay. Regrettably, compared to H1975 cells, H1975/OsiR cells exhibited less sensitivity to the tested ACC inhibitors (Fig. 5B). This might due to altered FASyn metabolism or multi-drug resistance, which needs to be further studied.

4. Discussion

A number of cancers exhibit an increase in *de novo* fatty acid synthesis (FASyn). The elevated FASyn in cancers is reflected by the upregulation of lipogenic enzymes, including ACC1, fatty acid synthase (FASN) and ATP citrate lyase (ACLY). In the present study, we found the mRNA levels of *ACC1* are increased in NSCLC patients, consistent with the previous findings in breast, liver and prostate cancers (Chin et al., 2006; Swinnen et al., 2000). Moreover, by using public database, we revealed that higher *ACC1* levels are associated with shorter PFS in NSCLC patients, suggesting that ACC1 might be a potential prognostic biomarker for NSCLC.

ND-646 is an allosteric inhibitor of ACC, with a unique mechanism of action. It binds to the BC domain of ACC, where the AMPK phosphorylated serine of ACC interacts to prevent dimerization and activation of ACC (Svensson and Shaw, 2016; Svensson et al., 2016), leading to constitutive dephosphorylation of ACC. Therefore, the phosphorylation status of ACC was used as a biomarker to evaluate how **ND-646** acted. Our synthesized derivatives of **ND-646** seemed to act with the same mechanism as **ND-646**, since compounds **A2**, **A7** and **A9** diminished the ACC phosphorylation as **ND-646** did.

Blockage of cancer cell FASyn by genetical or pharmacological targeting of lipogenic enzymes caused a marked decrease of lipogenesis and consequently cell growth arrest and apoptosis or autophagy depending on cancer cell types (Chajes et al., 2006; Svensson and Shaw, 2016). Our synthesized ACC1 inhibitors, **A2**, **A7** and **A9** as well as **ND-646**, indeed caused A549 NSCLC growth inhibition and cell death. However, the anti-cancer mechanism of ACC1 inhibitors has not been fully elucidated. Fatty acids not only supply with building blocks for synthesis of membranes during cell division by conversion into phospholipids (Stoiber et al., 2018), but also function as signaling molecules that trigger physiological responses directly or through lipidation of proteins, *e.g.*, WNT and Hedgehog (Petrova et al., 2017). Therefore, ACC1 inhibition might cause comprehensive influence to cancer cells, including effects on cellular membranes and numerous signaling pathways that link to proliferation and survival.

In conclusion, we for the first time verified that *ACC1* mRNA was upregulated in NSCLC and higher *ACC1* level was correlated with poor outcome in lung cancer patients, indicating ACC1 might be as a prognostic index for NSCLC patients. Moreover, we identified a series of ACC1 inhibitors with IC_{50} values from 2 nM to 25 nM. Compounds **A2**, **A7** and **A9** displayed strong cancer inhibitory activity in A549 cells by impairing cell growth and inducing cell death. These compounds are worth further evaluation for NSCLC treatment. Evaluation of a new concept of combination therapy with them as well as their safety profiles will be conducted in the coming future and results will be published elsewhere.

Credit author statement

C.P. Chen and X. Wen contribute to conceptualization, project administration, funding acquisition, manuscript writing and editing; C.P. Chen, E.Q. Li, W. Zhao, C. Zhang, L.Z. Qin, S.J. Liu, and Z.Q. Feng contribute to data curation, formal analysis, investigation, methodology and writing review; E.Q. Li and C.P. Chen wrote the original draft; W. Zhao and C. Zhang contribute to resources.

Acknowledgements

This work was supported by grants from the National Natural Science Foundation of China (grants 31501182, 81773584); Fundamental Research Funds for the Central Universities (2632017ZD05) and the scientific research fund for new teacher of

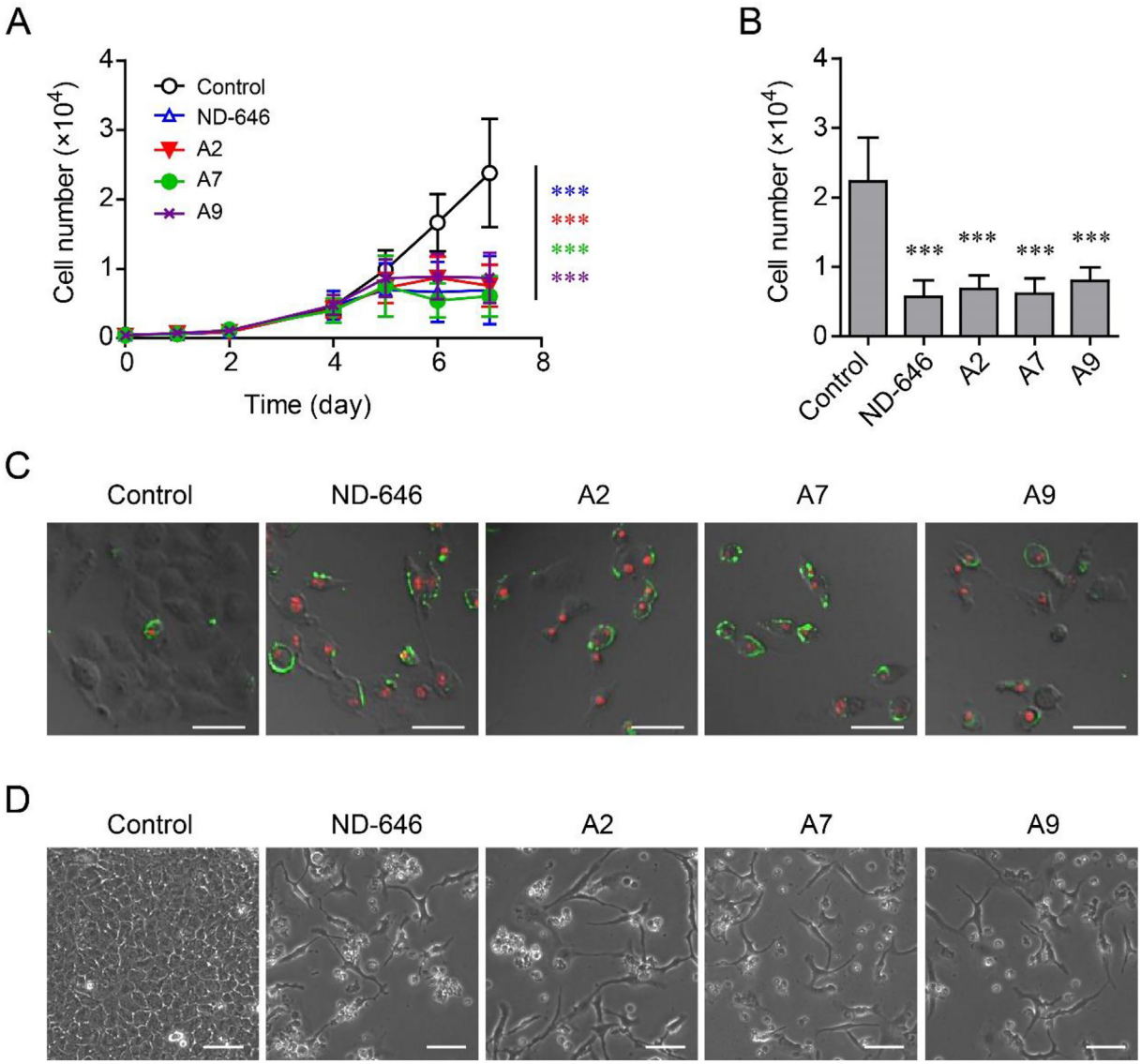

Fig. 4. Effects of ACC1 inhibitors on A549 cell growth and cell death. (A-B) Growth assay of A549 cells that were grown in delipidated FBS with 1 μM of ACC inhibitors for 7 days. Cell numbers were measured using the Opera Phenix system through digital phase contrast imaging (A) or DAPI staining toward the end treatment (B). Experiments were performed in sextuplicate. Statistical differences of cell numbers were calculated toward the end treatment. ***$P < 0.001$ (Student's *t*-test). (C) Cell death were analyzed by annexin V/PI staining after ACC1 inhibitors treatment for 7 days. Annexin V, PI and cell morphology were visualized with FITC (green), Alexa 568 (red) and brightfield respectively. Scale bars = 50 μm (D) Representative microphotographs of A549 cells cultured in regular FBS after receiving with ACC1 inhibitors (1 μM) for 12 days. Extensive cell death were seen after ACC1 inhibitors treatment. Scale bars = 75 μm. (For interpretation of the references to colour in this figure legend, the reader is referred to the web version of this article.)

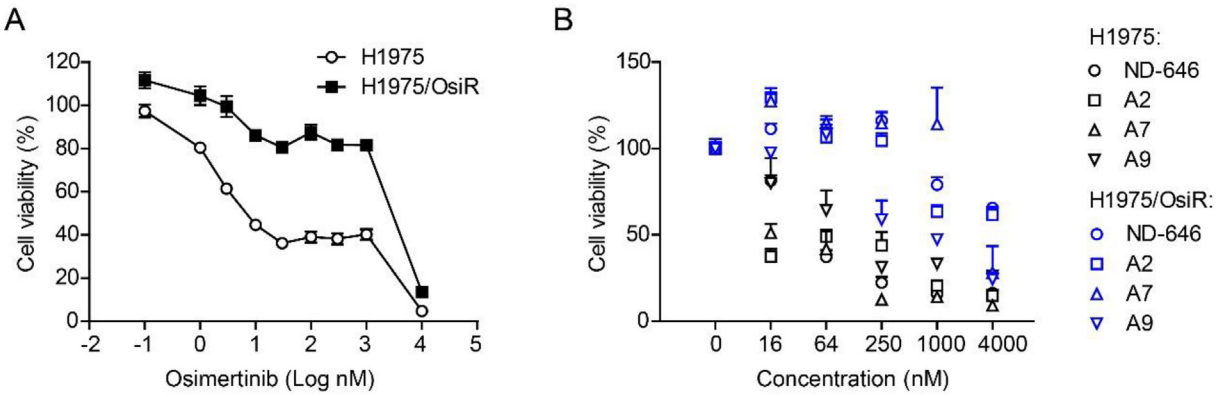

Fig. 5. Osi-resistant H1975 cells were less sensitive to ACC inhibitors. (A) Establishment of Osi-resistant H1975 cells. (B) Inhibitory effects of **ND-646**, **A2**, **A7** and **A9** in H1975 cells and H1975/OsiR cells.

China Pharmaceutical University.

Declaration of Competing Interest

The authors declare no conflict of interest.

Appendix A. Supplementary data

Supplementary data to this article can be found online at https://doi.org/10.1016/j.ejps.2019.105010.

References

Beckers, A., Organe, S., Timmermans, L., Scheys, K., Peeters, A., Brusselmans, K., et al., 2007. Chemical inhibition of acetyl-CoA carboxylase induces growth arrest and cytotoxicity selectively in cancer cells. Cancer Res. 67, 8180–8187.

Braig, S., 2018. Chemical genetics in tumor lipogenesis. Biotechnol. Adv. 36, 1724–1729.

Brusselmans, K., De Schrijver, E., Verhoeven, G., Swinnen, J.V., 2005. RNA interference-mediated silencing of the acetyl-CoA-carboxylase-alpha gene induces growth inhibition and apoptosis of prostate cancer cells. Cancer Res. 65, 6719–6725.

Cairns, R.A., Mak, T.W., 2016. The current state of cancer metabolism FOREWORD. Nat. Rev. Cancer 16, 613–614.

Carretero, J., Medina, P.P., Blanco, R., Smit, L., Tang, M., Roncador, G., et al., 2007. Dysfunctional AMPK activity, signalling through mTOR and survival in response to energetic stress in LKB1-deficient lung cancer. Oncogene 26, 1616–1625.

Chajes, V., Cambot, M., Moreau, K., Lenoir, G.M., Joulin, V., 2006. Acetyl-CoA carboxylase alpha is essential to breast cancer cell survival. Cancer Res. 66, 5287–5294.

Chen, C.P., Chen, X., Qiao, Y.N., Wang, P., He, W.Q., Zhang, C.H., et al., 2015. In vivo roles for myosin phosphatase targeting subunit-1 phosphorylation sites T694 and T852 in bladder smooth muscle contraction. J. Physiol. 593, 681–700.

Chen, C.P., Chen, K., Feng, Z., Wen, X., Sun, H., 2019. Synergistic antitumor activity of artesunate and HDAC inhibitors through elevating heme synthesis via synergistic upregulation of ALAS1 expression. Acta Pharm. Sin. B. https://doi.org/10.1016/j.apsb.2019.05.001.

Chin, K., DeVries, S., Fridlyand, J., Spellman, P.T., Roydasgupta, R., Kuo, W.L., et al., 2006. Genomic and transcriptional aberrations linked to breast cancer pathophysiologies. Cancer Cell 10, 529–541.

Currie E, Schulze A, Zechner R, Walther TC, Farese RV, Jr. Cellular fatty acid metabolism and cancer. Cell Metab. 2013;18:153–61.

Gyorffy, B., Surowiak, P., Budczies, J., Lanczky, A., 2013. Online survival analysis software to assess the prognostic value of biomarkers using transcriptomic data in non-small-cell lung cancer. PLoS One 8, e82241.

Harriman, G., Greenwood, J., Bhat, S., Huang, X., Wang, R., Paul, D., et al., 2016. Acetyl-CoA carboxylase inhibition by ND-630 reduces hepatic steatosis, improves insulin sensitivity, and modulates dyslipidemia in rats. Proc. Natl. Acad. Sci. U. S. A. 113, E1796–E1805.

Harriman, G.C., Masse, C.E., Harwood, J., Bhat, S., Greewood, J.R., 2013. Acetyl-CoA carboxylase inhibitors and uses thereof. World intellectual property organization (WO 2013/071169 A1).

Hou, J., Aerts, J., den Hamer, B., van Ijcken, W., den Bakker, M., Riegman, P., et al., 2010. Gene expression-based classification of non-small cell lung carcinomas and survival prediction. PLoS One 5, e10312.

Huang, W.Y., Hsu, S.D., Huang, H.Y., Sun, Y.M., Chou, C.H., Weng, S.L., et al., 2015. MethHC: a database of DNA methylation and gene expression in human cancer. Nucleic Acids Res. 43, D856–D861.

Huang, Y., Sun, G., Wang, P., Shi, R., Zhang, Y., Wen, X., et al., 2018. Synthesis and biological evaluation of complex I inhibitor R419 and its derivatives as anticancer agents in HepG2 cells. Bioorg. Med. Chem. Lett. 28, 2957–2960.

Jiang, W., Cai, G., Hu, P.C., Wang, Y., 2018. Personalized medicine in non-small cell lung cancer: a review from a pharmacogenomics perspective. Acta Pharm. Sin. B 8, 530–538.

Lally, J.S.V., Ghoshal, S., DePeralta, D.K., Moaven, O., Wei, L., Masia, R., et al., 2019. Inhibition of acetyl-CoA carboxylase by phosphorylation or the inhibitor ND-654 suppresses lipogenesis and hepatocellular carcinoma. Cell Metab. 29 (1), 174–182.

Liu, Z., Li, Q., Liu, R., Zhao, G., Zhang, Y., Zheng, M., et al., 2016. Expression and methylation of microsomal triglyceride transfer protein and acetyl-CoA carboxylase are associated with fatty liver syndrome in chicken. Poult. Sci. 95, 1387–1395.

Martinez-Outschoorn, U.E., Peiris-Pages, M., Pestell, R.G., Sotgia, F., Lisanti, M.P., 2017. Cancer metabolism: a therapeutic perspective. Nat. Rev. Clin. Oncol. 14, 113.

McGarry, J.D., Leatherman, G.F., Foster, D.W., 1978. Carnitine palmitoyltransferase I. the site of inhibition of hepatic fatty acid oxidation by malonyl-CoA. J. Biol. Chem. 253, 4128–4136.

Medes, G., Thomas, A., Weinhouse, S., 1953. Metabolism of neoplastic tissue. IV. A study of lipid synthesis in neoplastic tissue slices in vitro. Cancer Res. 13, 27–29.

Menendez, J.A., Lupu, R., 2007. Fatty acid synthase and the lipogenic phenotype in cancer pathogenesis. Nat. Rev. Cancer 7, 763–777.

Okayama, H., Kohno, T., Ishii, Y., Shimada, Y., Shiraishi, K., Iwakawa, R., et al., 2012. Identification of genes upregulated in ALK-positive and EGFR/KRAS/ALK-negative lung adenocarcinomas. Cancer Res. 72, 100–111.

Petrova, E., Scholz, A., Paul, J., Sturz, A., Haike, K., Siegel, F., et al., 2017. Acetyl-CoA carboxylase inhibitors attenuate WNT and hedgehog signaling and suppress pancreatic tumor growth. Oncotarget 8, 48660–48670.

Portela, A., Esteller, M., 2010. Epigenetic modifications and human disease. Nat. Biotechnol. 28, 1057–1068.

Rios Garcia, M., Steinbauer, B., Srivastava, K., Singhal, M., Mattijssen, F., Maida, A., et al., 2017. Acetyl-CoA carboxylase 1-dependent protein acetylation controls breast Cancer metastasis and recurrence. Cell Metab. 26, 842–855 (e5).

Romaniello, D., Mazzeo, L., Mancini, M., Marrocco, I., Noronha, A., Kreitman, M., et al., 2018. A combination of approved antibodies overcomes resistance of lung Cancer to Osimertinib by blocking bypass pathways. Clin. Cancer Res. 24, 5610–5621.

Song, Z., Chen, C.P., Liu, J., Wen, X., Sun, H., Yuan, H., 2016. Design, synthesis, and biological evaluation of (2E)-(2-oxo-1, 2-dihydro-3H-indol-3-ylidene)acetate derivatives as anti-proliferative agents through ROS-induced cell apoptosis. Eur. J. Med. Chem. 124, 809–819.

Stoiber, K., Naglo, O., Pernpeintner, C., Zhang, S., Koeberle, A., Ulrich, M., et al., 2018. Targeting de novo lipogenesis as a novel approach in anti-cancer therapy. Br. J. Cancer 118, 43–51.

Svensson, R.U., Shaw, R.J., 2016. Lipid synthesis is a metabolic liability of non-small cell lung cancer. Cold Spring Harb. Symp. Quant. Biol. 81, 93–103.

Svensson, R.U., Parker, S.J., Eichner, L.J., Kolar, M.J., Wallace, M., Brun, S.N., et al., 2016. Inhibition of acetyl-CoA carboxylase suppresses fatty acid synthesis and tumor growth of non-small-cell lung cancer in preclinical models. Nat. Med. 22, 1108–1119.

Swinnen, J.V., Vanderhoydonc, F., Elgamal, A.A., Eelen, M., Vercaeren, I., Joniau, S., et al., 2000. Selective activation of the fatty acid synthesis pathway in human prostate cancer. Int. J. Cancer 88, 176–179.

Vander Heiden, M.G., Cantley, L.C., Thompson, C.B., 2009. Understanding the Warburg effect: the metabolic requirements of cell proliferation. Science 324, 1029–1033.

Wang, C., Ma, J., Zhang, N., Yang, Q., Jin, Y., Wang, Y., 2015. The acetyl-CoA carboxylase enzyme: a target for cancer therapy? Expert. Rev. Anticancer. Ther. 15, 667–676.

Zadra, G., Ribeiro, C.F., Chetta, P., Ho, Y., Cacciatore, S., Gao, X., et al., 2019. Inhibition of de novo lipogenesis targets androgen receptor signaling in castration-resistant prostate cancer. Proc. Natl. Acad. Sci. U. S. A. 116, 631–640.